First-principles investigation of N–Ag co-doping effect on electronic properties in p-type ZnO

Zuo Chun-Ying(左春英)[a)], Wen Jing(温 静)[a)], and Bai Yue-Lei(柏跃磊)[b)]

[a)] *Arts and Science Department of Heilongjiang August First Land Reclamation University, Daqing* 163319, *China*
[b)] *Center for Composite Materials and Structures, Harbin Institute of Technology, Harbin* 150080, *China*

(Received 3 July 2009; revised manuscript received 3 November 2009)

The geometric structure, band structure and density of states of pure, Ag-doped, N-doped, and N–Ag codoped wurtzite ZnO have been investigated by the first-principles ultra-soft pseudopotential method based on the density functional theory. The calculated results show that the carrier concentration is increased in the ZnO crystal codoped by N and Ag, and the codoped structure is stable and is more in favour of the formation of p-type ZnO.

Keywords: first-principles, co-doping, ZnO, electronic properties

PACC: 7115A, 7115M, 7115H

1. Introduction

Wurtzite-ZnO, a wide-gap (E_g = 3.37 eV) semiconductor,[1−3] is widely used in electronic and photonic materials, and has great potential applications in information technology, biotechnology, and nanoscale science and engineering.[4−8]

In particular, ZnO is a new hot research topic in the field of short-wavelength semiconductors after GaN.[9,10] However, the realisation of stable and reproducible p-type ZnO with acceptable carrier concentration and low resistivity has been the bottleneck of ZnO-based optoelectronic devices.[6,11−13] It is difficult to fabricate p-type ZnO because it is a material having only n-type conduction due to a large number of native defects, such as oxygen vacancies and zinc interstitials.[14,15] If we want ZnO-based devices, such as light emitting diodes and optical masers, to be made successfully, fabrication of p-type ZnO and p–n junctions with the same properties is the crucial problem.

The p-type doping is a possible method using different forms of dopant sources, for example, group-I elements such as Li and Na; group-V elements such as N, P and As; and group-IB elements such as Ag.[16−23] However, it is still difficult to fabricate high-quality ZnO because the acceptor level of group-V elements is so deep that it is difficult to activate the effective acceptors; group-I elements such as Li and Na tend to occupy the interstitial sites, which leads to self-compensation although their acceptor level is not deeper. Also, p-type ZnO is difficult to gain in Ag-doped ZnO because Ag behaves like a deeper acceptor.[23]

The problems of ZnO codoped by N and Ag including model IV and model V as described in this paper are analysed, and research, from the viewpoint of the microscopic mechanism, is done on its lattice parameters, band structure and density of states. The related experimental results[24] confirm that high carrier concentration is obtained by the double acceptor codoping of N and Ag. But theoretical research about this has not been reported yet.

2. Computational method and theoretical model

2.1. Theoretical model

ZnO of groups II–VI is a promising semiconductor material with direct wide band gap, the stable phase of which belongs to the hexagonal wurtzite structure at ambient temperature and pressure. ZnO belongs to $P63mc$ space group, with lattice parameters $a = b = 0.3247$ nm, $c = 0.5203$ nm, $c/a = 1.602$.

The supercell (2×2×1) employed contains 8 oxygen atoms and 8 zinc atoms. The supercell models used in computation are pure ZnO (model I), ZnO with one Zn replaced by one Ag (model II), ZnO with one O replaced by one N (model III), ZnO with one Zn and one O replaced respectively by one Ag and one N (models IV and V). The structures of the supercell are shown in Fig. 1.

© 2010 Chinese Physical Society and IOP Publishing Ltd

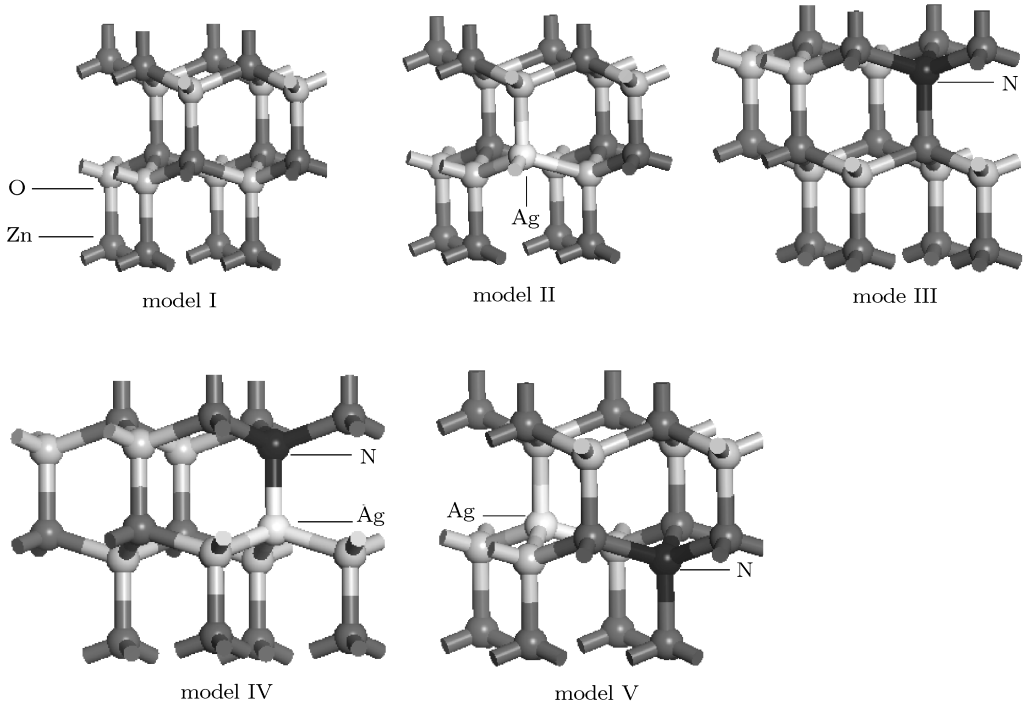


Fig. 1. The structures of the un-doped and doped ZnO wurtzite supercell.

2.2. Computational method

The calculations were carried out using the CASTEP software package,[25] which is an *ab initio* molecular dynamics program in Materials Studio based on the density functional theory (DFT) and pseudopotential plane wave.[26] The exchange and correlation interactions were treated within the framework of the generalised gradient approximation (GGA).[27] The potentials among ion core and valence electrons were described by ultra-soft pseudopotentials (USPs),[28] and valence-electron configurations are: Zn-$3d^{10}4s^2$, O-$2s^22p^4$, N-$2s^22p^3$, Ag-$4d^{10}5s^1$. Special k points of 8×8×6 were employed, together with an energy cutoff of the plane wave of 360 eV.

3. Results and discussion

3.1. Investigation of the stability of the structures

The structures of un-doped and doped ZnO wurtzite supercells were optimised in order to determine the influence of impurity on the stability of the structure. Firstly, supercell structures were optimised, from which lattice parameters were obtained, then internal coordinates were optimised to obtain the exact results. Band structure and the density of states were computed after the geometry optimization. The results are listed in Table 1.

Table 1. Structure parameters after geometry optimisation (units in nm for a, c and bond length and nm^3 for volume).

material	a		c		c/a		bond length		volume
	Expt.	Calc.	Expt.	Calc.	Expt.	Calc.	c-axis	un-c-axis	
ZnO (model I)	0.32465	0.32975	0.5203	0.52861	1.60	1.60	0.2015	0.2005	0.1991
ZnO: Ag (model II)	0.32465	0.33407	0.5203	0.54197	1.60	1.62	0.2315	0.2233	0.2095
ZnO: N (model III)	0.32465	0.32901	0.5203	0.52965	1.60	1.61	0.1951	0.1960	0.1986
ZnO: Ag, N (model IV)	0.32465	0.33761	0.5203	0.52684	1.60	1.56	0.2176	Ag-O: 0.2237 N-Zn: 0.2001	0.2080
ZnO: Ag, N (model V)	0.32465	0.33327	0.5203	0.54206	1.60	1.63	Ag-O: 0.1983 N-Zn: 0.1983	Ag-O: 0.1974 N-Zn: 0.1974	0.2086

Table 1 shows that the lattice parameters of doped crystal of a (except for model III) and c (except for model IV) are larger than those of the undoped ZnO. It is seen clearly that the cell volume of ZnO is swollen after Ag- and N+Ag-doping in ZnO, but that of N-doped ZnO is reduced slightly.

As for pure ZnO crystal structure, the calculated lattice parameters a and c are slightly larger than the experimental results and c/a is in good agreement with the experimental data, which shows that the computation method is reliable.

The radius of Ag^+(0.126 nm) is longer than that of Zn^+ (0.074 nm) when Ag is occupying the Zn site, which leads to the increasing volume of model II.

As illustrated in Table 1, the lattice structure of ZnO doped by N alone has nearly no change. Although the ionic radius of N[29] (0.146 nm) and covalent radius of N (0.075 nm) are both longer than those of O^{2-} (0.132 nm) and O (0.073 nm) respectively, the proportion of the covalent bond to the chemical bond is larger for the N–Zn bond than for the O–Zn bond according to population analysis. That is why the volume of ZnO when N is occupying the O site is a little reduced, which is consistent with experimental results.[30]

Table 1 shows that the cell volume of ZnO codoped by N and Ag is slightly smaller than that of ZnO doped by Ag, but larger than that of pure ZnO. The reason is that the repulsion potential between the localised negative electricity core, formed when Zn is replaced by Ag, and the neighbouring O atoms is comparatively larger than the attraction potential between the localised negative electricity core, formed when O is replaced by N, and the neighbouring Zn atoms. This is verified by the fact that the bond length of Ag–O is longer than those of Zn–O and Zn–N.

The final energies of two codoped models have been computed in this paper, in which model IV is more stable because its final energy (−16325.21 eV) is smaller than that of model V (−16324.76 eV).

3.2. Electronic structure of ZnO

Comparing with the electronic structure of doped ZnO semiconductor, the density of states (DOS) including total DOS, partial DOS (PDOS) and the band structure of the undoped ZnO were firstly calculated after geometry optimisation. The calculated results are shown in Figs. 2 and 3, which are in agreement with the results calculated using other theoretical methods.[31−33]

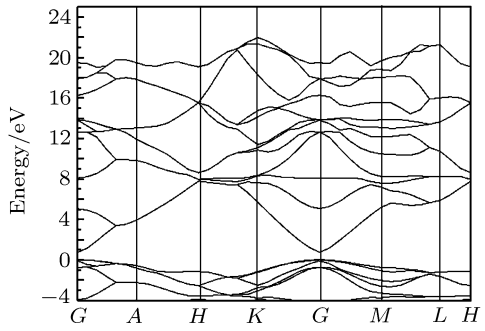


Fig. 2. Band structure of pure ZnO.

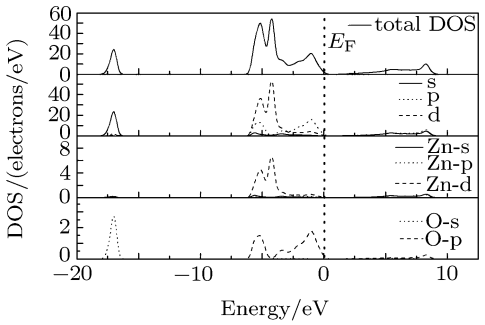


Fig. 3. DOS of pure ZnO.

Figure 2 shows the band structure of pure ZnO. The direct band gap is about 0.76 eV at the highly symmetric $G(\Gamma)$ point, which is in accordance with other computed values using DFT, such as 0.73 eV by Schleife[34] and 0.80 eV by Janotti;[35] and it is far less than the experimental value of 3.37 eV. It is well known that the underestimated band gap can be due to neglect of correlation between excited-state electrons. It is meaningful to study the variations of band gap in doped ZnO under the same computational condition by using DFT. The lower valence band from mainly Zn-3d changes slowly because the 3d states of Zn are full of electrons. Compared with the conduction band from Zn-4s, the gentle change of the upper valence band from the O-2p illustrates that the holes in the valence band have a biggish effective mass, which is one of the main reasons for the difficulty in realisation of p-type ZnO.[36]

For undoped ZnO, figure 3 shows that there are two groups in the valence band. The upper valence band (−4.04–0.01 eV) originates mainly from 2p states at O sites with a small contribution from 3d states at Zn sites; the lower valence band (−6.22–−4.04 eV) with a strong d character is mainly composed of 3d

states at Zn sites. The conduction band comes mainly from the 4s states at Zn sites and 2p states at O sites. The narrow valence band region located at −17.32 eV resulting from the 2s states at O sites is not discussed because of its weak interaction with other electron states.

3.3. Results and discussion on Ag-doped ZnO

When a Zn atom is replaced by the Ag atom in model II, its doping concentration is 12.50%. The band structure and DOS for ZnO crystal doped by Ag are shown in Figs. 4 and 5. It is obvious that a newly occupied band appears near the top of the valance band which is a deep acceptor level of 0.51 eV close to the earlier calculated results.[23,37] It is for this reason that the formation of holes in the valence band needs much activation energy which induces the low concentration of the holes and suppresses the formation of p-type ZnO in Ag-doped materials.

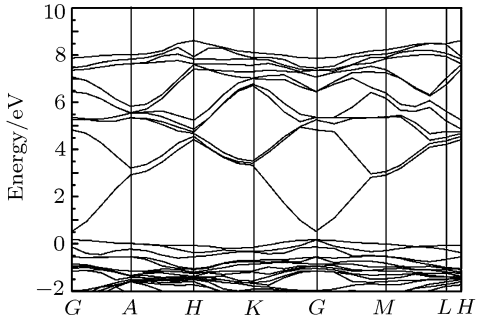


Fig. 4. Band structure of Ag-doped ZnO.

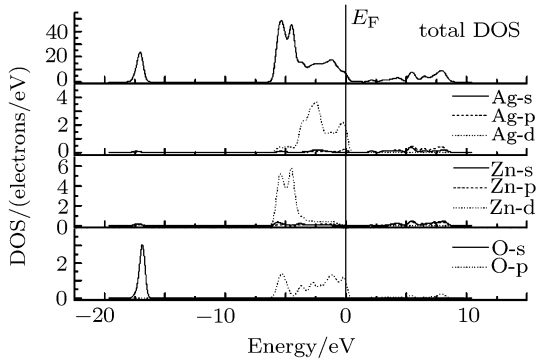


Fig. 5. DOS of Ag-doped ZnO.

It can be seen clearly from Fig. 5 that there is an impurity peak near the Fermi level when the Ag occupies the Zn site and it is possible to form the p-type ZnO by the Fermi level moving into the valence band. The impurity peak mainly comes from Ag-4d and O-2p states shown by PDOS of Ag, O, and Zn. The appearance of the acceptor impurity peak at the top of valence band is induced by orbital overlap between Ag-4d and O-2p whose energy increases slightly due to the doping of Ag. It is the Ag displacement that causes the cleavage strength of the 2p peak to become stronger.

The density of states of the Ag atom near the Fermi level is bigger than those of the other atoms, which is helpful for the formation of p-type ZnO and yet the strong localisation of the acceptor restricts p-type doping.

3.4. Results and discussion on N-doped ZnO

The band structure, the total DOS and the PDOS of N, the nearest-neighbour Zn and the next-nearest-neighbour O are illustrated in Figs. 6 and 7. The results are consistent with those in Ref. [38]. A strong localised energy band located at approximately −12.98 eV which comes from N-2s states is omitted in Fig. 6 because such electrons have little interaction with other states.

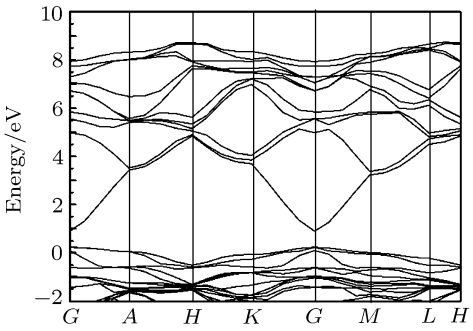


Fig. 6. Band structure of N-doped ZnO.

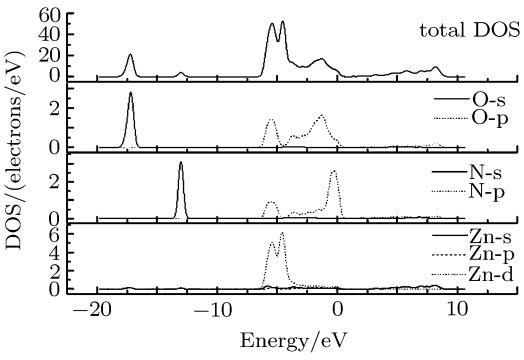


Fig. 7. DOS of N-doped ZnO.

There are excess carriers (holes) near the top of the valence band, which originate mainly from p states

at N sites with a little O-2p effect. The number of DOS for 2p states of O at the Fermi level around Ag and N for model II and model III reach about 0.90 and 0.34 respectively, therefore in model III, the acceptor level is so localised that the repulsive interaction becomes the strongest among the acceptors, thus reducing the solid solubility of N and increasing the system energy. That is the reason why it is difficult to form p-type ZnO. The orbital energy of 2p states of O shifts to a higher energy value for model III because N is easier to obtain electrons from the neighbouring O atoms and the common movement is strengthened for the orbital hybridisation effect occurring among p states of O and N sites. Since the PDOS of Zn in model III is similar to that of pure ZnO, the cleavage strength of the 3d peak in the lower valence band is weaker for this model; furthermore, the DOS of the nearest-neighbour of Zn near the Fermi level becomes dispersed after the impurity is added into the pure ZnO. The conduction band still consists mainly of 2p states of O and 4s states of Zn. There are fewer carriers by replacing O by N.

3.5. Analysis of electronic structure of codoped ZnO

Two kinds of N+Ag codoped ZnO structures are computed as for model IV and model V. It is seen clearly from Table 1 that the cell volume of these two models is almost the same; however, model IV is more stable because its final energy (−16325.21 eV) is smaller than that of model V (−16324.76 eV). The Fermi level moves deeply into the valence band of the two models. In model IV and model V the values of integral DOS attained are 2.02 and 2.22 respectively according to the DOS being integrated from the Fermi level to the valence band maximum (VBM), which confirms that there are more carriers provided by the model V. Exact band gaps are 0.21 eV for model IV and 0.42 eV for model V. The carrier concentration is increased, the electrical resistivity is reduced and the conductivity is improved for wurtzite ZnO codoped by N and Ag. Next, the model IV is analysed specifically.

The values of DOS are 1.94, 1.69, 2.02 and 2.22 respectively for the models II to V, which are calculated by the integration over the values from the Fermi level to the VBM and the values of total DOS are 144.45, 128.26, 144.08 and 144.29 respectively, which are obtained by integration over the whole valence band. We see that it is helpful to form p-type ZnO by codoping of N and Ag.

The energy band and the DOS for model IV are illustrated in Figs. 8 and 9. The band gap of N+Ag codoped ZnO is the narrowest and its red-shift phenomenon is the most obvious one among the three doped models. One strongly localised band located at −13.22 eV is mainly from the 2s states of N according to comparison with pure ZnO; however, the band shifts to lower energy when contrasted with the N-doped crystal.

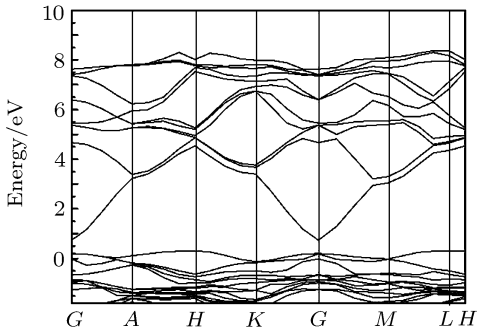


Fig. 8. Band structure of model IV.

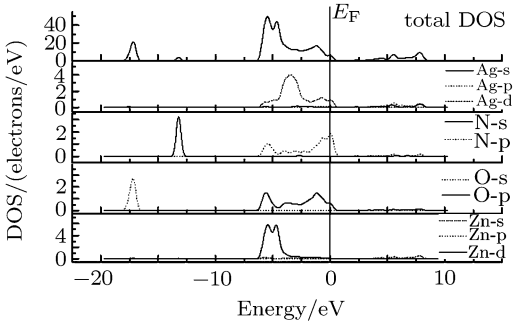


Fig. 9. DOS of model IV.

Therefore, to understand the reason why the bands change, the electronic structure of the codoped semiconductor ZnO is analysed intensively. Compared with pure ZnO, there are still contributions from 4d states of Ag and 2p states of N besides 2p states of O in VBM, and there are little contributions from the 5s states of Ag besides the 4s states of Zn in the conduction band maximum (CBM). The band gap reduces 0.55 eV compared with the pure ZnO due to the fact that VBM shifts to the higher energy region and CBM moves into the lower one.

Doping one element or two elements shows a different effect on the electronic structure of the ZnO. The changes of electronic structure are analysed based on the codoped DOS graphs.

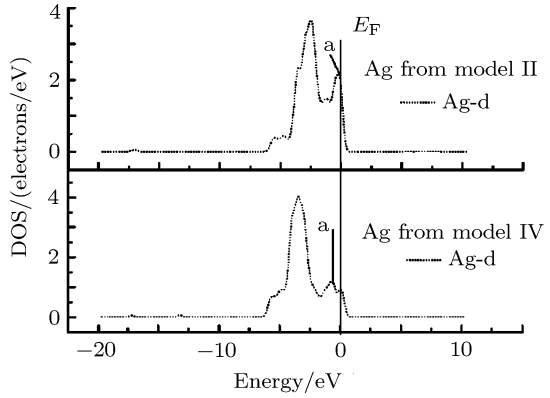


Fig. 10. PDOS of Ag for models II and IV.

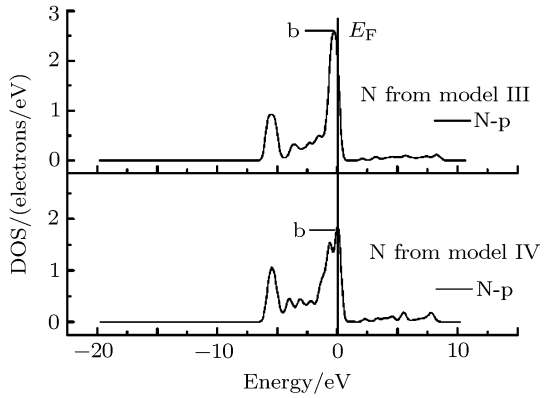


Fig. 11. PDOS of N of models III and IV.

It can be seen clearly from Fig. 10 that the PDOS of Ag in model IV is very similar to that of ZnO doped by Ag alone; however, it is obvious that the "a" peak width (2.51 eV) is broadened compared with the width (1.68 eV) in model II. Figure 11 shows that the 2p peak value of N is 1.85 and 2.58 for models IV and III respectively; at the same time, the "b" peak width is 2.74 eV and 1.99 eV respectively. Therefore, the localisation degree of the acceptor levels of N and Ag is minimised, the solid solubility is improved, at the same time, the acceptor level of Ag (0.35 eV) becomes shallower. The reasons are as follows: firstly, the orbital hybridisation of 4d states of Ag and the lower energy region makes it shift to the lower energy region; secondly, when Zn is replaced by Ag, the common movement of electrons is strengthened because the holes are not only limited to Ag, but also act on neighbouring N atoms.

Comparing model IV with the other models, the basic configuration of PDOS of Zn is unchanged because the interaction between Zn atoms and the impurity atom is very weak. The peak of the upper valence band from 2p states at O sites shows a splitting phenomenon as compared with pure ZnO.

The Fermi level moves deeply into the valence band of Zn and O for model V (Zn: 0.83 eV, O: 0.98 eV) as shown in Fig. 12 compared with the other models. This shows that the holes are not limited to N and Ag, but act on their neighbouring Zn and O atoms. There are two reasons for the results. The first is that the common movement of electrons from the 2p states of N and 4d states of Zn becomes stronger; the second is that there is a stronger orbital hybridisation interaction between the 2p states of O and 4d states of Ag.

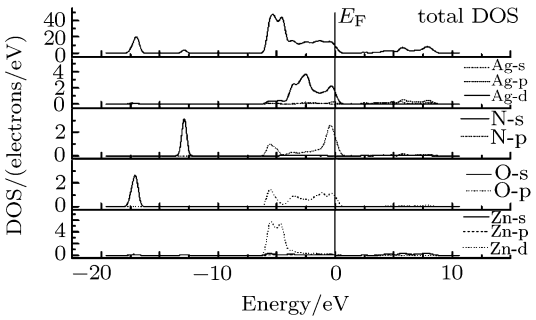


Fig. 12. DOS of model V.

4. Conclusion

In summary, using the first-principles calculation of plane wave ultra-soft pseudopotential technology based on the density functional theory, we have investigated the geometry structure, band structure and density of states of undoped and doped ZnO. We find that the solid solubility of ZnO doped by double acceptors can be improved due to the two impurities activating each other. Compared with model V, model IV is more stable because it has less total energy. However, there are more carriers for model V because the common movement of electrons among the impurities of N and Ag and their neighbouring Zn and O atoms is stronger.

In conclusion, the present results indicate that the carrier concentration is improved in N+Ag codoped ZnO, and this is helpful to form p-type ZnO.

Acknowledgments

The authors thank Prof. Zhu J C (Harbin Institute of Technology) for providing the software resource — CASTEP. The authors would like to thank Prof. Duan Man-Yi (Sichuan Normal University) for useful discussion during the course of this study. We thank PhD Zhong Cheng (College of Chemistry and Molecular Sciences of Wuhan University) for his kind encouragement and technical support during the calculation.

References

[1] Zhang X D, Guo M L, Liu C L, Zhang L A, Zhang W Y, Ding Y Q, Wu Q and Feng X 2008 *Physical Journal* B **62** 417
[2] Shen Y B, Zhou X, Xu M, Ding Y C, Duan M Y, LingHu R F and Zhu W J 2007 *Acta Phys. Sin.* **56** 3440 (in Chinese)
[3] Yang Y T, Wu J, Cai Y R, Ding R X, Song J X and Shi L C 2008 *Acta Phys. Sin.* **57** 7151 (in Chinese)
[4] Alivov Y I, Look D C, Ataev B M, Chukichev M V, Mamedov V V, Agafonov Y A and Pustovit A N 2004 *Solid State Electron.* **48** 2343
[5] Makino T, Chia C H, Tuan N T and Segawa Y 2000 *Appl. Phys. Lett.* **77** 1632
[6] Look D C 2001 *Mater. Sci. Eng.* B **80** 383
[7] Zhang F Y, You J Q, Zeng Z and Zhong G H 2007 *Chin. Phys.* **16** 3815
[8] Zhang F C, Zhang Z Y, Zhang W H, Yan J F and Yong J N 2009 *Chin. Phys.* B **18** 2508
[9] Gupta A, Verma N K and Bhatti H S 2007 *J. Low Temp. Phys.* **14** 749
[10] Yoshino K, Hata T, Kakeno T, Komaki H, Yoneta M, Akaki Y and Ikari T 2003 *Phys. Stat. Sol.* (c) **0** 626
[11] Özgür Ü, Alivov Y I, Liu C, Teke A, Reshchikov M A and Morkoc H 2005 *J. Appl. Phys.* **98** 041301
[12] Look D C, Claflin B and Alivov Y I 2004 *Phys. Status Solidi* **201** 2203
[13] Look D C and Claflin B 2004 *Phys. Status Solidi* **241** 624
[14] Zhang J K, Deng S H and Jin H 2007 *Acta Phys. Sin.* **56** 537 (in Chinese)
[15] Wang J W, Bian J M, Sun J C, Liang H W, Zhao J Z and Du G T 2008 *Acta Phys. Sin.* **57** 5212 (in Chinese)
[16] Ryu Y R, Zhu S and Look D C 2000 *Crystal Growth* **216** 330
[17] Hwang D K, Oh M S, Lim J H, Kang C G and Park S J 2007 *Appl. Phys. Lett.* **90** 021106
[18] Tu M L, Su Y K and Ma C Y 2006 *J. Appl. Phys.* **100** 053705
[19] Wang X, Lu Y M, Shen D Z, Zhang Z Z, Li B H, Yao B, Zhang J Y, Zhao D X and F X W 2006 *Chin. J. Lumin.* **27** 426 (in Chinese)
[20] Zhang X, Li X M, Chen T L, Yu W D, Gao X D, Zhang C Y and Zhao J L 2006 *Chin. J. Lumin.* **26** 503 (in Chinese)
[21] Wang X H, Yao B and Shen D Z 2006 *Chin J. Lumin.* **27** 946 (in Chinese)
[22] Zeng Y J, Ye Z Z, Xu W Z, Li D Y, Lu J G, Zhu L P and Zhao B H 2006 *Appl. Phys. Lett.* **88** 062107
[23] Wan Q X, Xiong Z H and Dai J N 2008 *Opt. Mater.* **30** 821
[24] Wang J W, Bian J M and Liang H W 2008 *Chin. Phys. Lett.* **25** 3400
[25] Segall M D, Lindan P J D, Probert M J, Pickard C J and Hasnip P J 2002 *J. Phys.: Condens. Matter.* **14** 2717
[26] Payne M C, Teter M P, Allan D C, Arias T A and Jornnopoulos J D 1992 *Rev. Mod. Phys.* **64** 1045
[27] Perdew J P, Burke K and Ernzerhof M 1996 *Phys. Rev. Lett.* **77** 3865
[28] Vanderbilt D 1990 *Phys. Rev.* B **41** 7892
[29] Chen K, Fan G H and Zhang Y 2008 *Acta Phys. Chim. Sin.* **24** 63 (in Chinese)
[30] Chen L L, Lu J G and Ye Z Z 2005 *Appl. Phys. Lett.* **87** 252106
[31] Zhang X D, Guo M L and Liu C L 2008 *Phys. J.* B **62** 418
[32] Sun J, Wang H T and He J 2005 *Phys. Rev.* B **71** 125132
[33] Yamamoto T 2002 *Thin Solid Films.* **420–421** 101
[34] Schleife A, Fuchs F, Furthmuller J and Bechstedt F 2006 *Phys. Rev.* B **73** 245212
[35] Janotti A, Segev D and Van de Walle C G 2006 *Phys. Rev.* B **74** 045202
[36] Chen K, Fan G H and Zhang Y 2008 *Acta Phys. Sin.* **57** 1056 (in Chinese)
[37] Yan Y F, Al-Jassim M M and Wei S H 2006 *Appl. Phys. Lett.* **89** 181912
[38] Harish K Y, Sreenivas K and Vinay G J 2006 *Appl. Phys.* **99** 83507